Modeling and Simulation of a Stiffness-controlled Micro-bridge Resonator

Fabrice Verjus, Tarik Bourouina, Eric Belhaire, Nicolas Mauduit, Alain Bosseboeuf.

Institut d'Electronique Fondamentale CNRS URA 022,
Université Paris XI Bât 220. 91405 Orsay, France.
Phone : + (33) (1) 69 15 40 01 Fax : + (33) (1) 69 15 40 00
Email: verjus@ief.u-psud.fr

ABSTRACT

This paper deals with the modeling and simulation of electrical stiffness control of a micro-bridge. Stiffness variations are obtained by compressive stresses that result from Joule heating. The micro-bridge is slaved to resonance in order to control its stiffness through its resonance frequency. This is carried-out in a PLL-based circuit in which the mechanical resonator acts as a VCO. Multi-level simulations have been achieved. A first-order analytical model of the micro-bridge has been set on the basis of approximations. Then, FEM simulations have been performed and used to build a refined model. The micro-bridge models have been implemented in HDLA language for the ELDO simulator. Finally, a system-level simulation has been used to analyze the behavior of the whole system, which includes the micro-bridge resonator linked with other electrical components.

Keywords: resonator, buckling, FEM analysis, HDLA, multi-level simulation

INTRODUCTION

Compliance control of mechanical microstructures opens ways to build devices endowed with attractive features, including tunable resonators and sensors with tunable dynamic range or with very high sensitivity. Electrostatically induced stiffness variations have already been demonstrated [1].

In this paper, we consider stiffness variations due to Joule heating. In addition to the applications mentioned above, this actuation principle allows new ones such as actuators with extended range of motion [2-4] or tunable wide-range resonators. This arises from the fact that large compressive stresses can be easily generated by Joule heating in a clamped-clamped structure. In particular, stresses corresponding to the buckling threshold and the post-buckling regime are attainable. Once the structure is buckled, the deflection increases with compression increasing -which suggests applications to actuators. The state preceeding buckling is characterized by a small stiffness, suggesting applications to sensors and wide-range frequency tuning.

An analytical model of a stressed micro-bridge has been established. This analytical model has been implemented in HDLA language for a subsequent use in the ELDO simulator. Finite Element Modeling (FEM) simulations with the ANSYS software have been performed to refine the analytical model and to test its accuracy.

An electronic circuit is necessary for the stiffness control. To do this, we have chosen to perform a control of the first bending resonance frequency. A first loop is used for the excitation of the resonator. A second loop, a Phase-Locked-Loop (PLL), including the mechanical resonator as a Voltage-Controlled-Oscillator (VCO), is used to set a working frequency, which is equivalent to choosing a desired stiffness (or a particular post-buckling position). A system-level simulation of this circuit which includes electrical components and the micro-bridge resonator has been performed in the ELDO simulator.

DEVICE STRUCTURE AND OPERATION PRINCIPLE

Principle of the electrically tunable mechanical resonator:

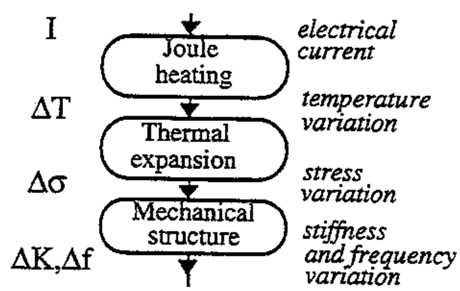

Figure 1
Stiffness control by Joule heating

The device under consideration is a clamped-clamped micro-bridge. This micro-bridge is used as a mechanical resonator whose frequency is tuned by an electrical current, according to the diagram shown in Fig.1. An electrical current I, flowing through the structure produces a temperature rise ΔT by Joule heating. As a consequence, a compressive stress $\Delta\sigma$ is generated in addition to the initial built-in stress σ_0, so that the total stress $\sigma=\Delta\sigma+\sigma_0$ acts as an axial load to the mechanical structure. Finally, the bending stiffness and the resonance frequency of the micro-bridge are affected by this stress change. From a mechanical point of vue, the device is a clamped-clamped structure submitted to the simultaneous action of an axial stress and a transversal vibration, the axial stress being of thermal nature and resulting from Joule heating.

Among the various vibration excitation and detection methods of mechanical resonators, we have chosen a solution which is compatible with the most common MEMS processes. It consists of electrostatic excitation and detection. A thermal actuation and a piezoresistive detection are also under consideration. The resonator structure can be fabricated either by electrodeposition through micro-moulds [5], or by deep RIE etching of patterns on SOI wafers, or by the SCREAM process [6]. An example of test device is shown in Fig.2.

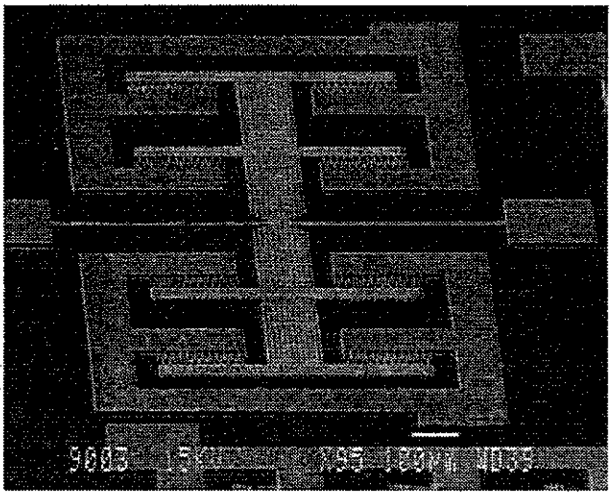

Figure 2
Test device: tunable micro-bridge resonator with Joule actuation and electrostatic excitation and detection

MICROSYSTEM MODELING AND SIMULATION

Typical microsystem simulations involve the following steps:
1) behavioral simulations at the device level. The characteristics of each elementary component are deduced for a subsequent use. These simulations can be performed either on the basis of analytic models or from numerical simulations.
2) behavioral simulations at the system level to analyze the whole system. These simulations can be performed in a SPICE-like tool including description capabilities of non-electrical analog components with complex characteristics (eg. ELDO/HDLA).
3) technological Computer-Aided Design (T-CAD) simulations.

Concerning the simulation of the electrically controlled micro-bridge resonator, we followed the procedure illustrated in Fig.3 in which appear the first two steps mentioned above. First, the behavior of the micro-bridge resonator was described by means of a set of equations, leading to a first-order analytical model. Then, numerical simulations were carried out with the help of a Finite Element Modeling (FEM) software (ANSYS) in order to build a refined model. Nonlinear static buckling and modal analyses were performed. (Thermal and electro-thermo-mechanical simulations are also under consideration to have a higher level of refinement and to account for interactions between the different fields). It is noteworthy that, for more complex geometries, an analytical model may be difficult to obtain. In those cases it would be necessary to resort directly to a numerical solution like FEM. Finally, a system-level simulation was performed to analyze the stiffness control through a frequency control. A PLL-based electrical circuit has been simulated in the ELDO simulator. The Voltage Controlled Oscillator (VCO) of this PLL has been substituted by the current controlled micro-bridge resonator considered in this paper. We have chosen to implement the first-order analytical model of this resonator through a HDLA description. This mechanical VCO has been linked to other conventional electrical components to constitute the PLL.

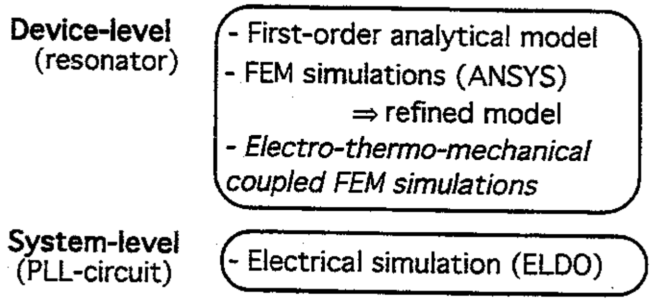

Figure 3
Modeling and simulation flow

ANALYTICAL MODEL OF THE MICRO-BRIDGE RESONATOR

1 - Stress induced stiffness variations

1.1 - Stress-free structure

For a stress-free micro-bridge with a rectangular cross section, the first bending resonance frequency f_{R0} and the bending stiffness k_0 are given by the following formulae [7]:

$$f_{R0} = 1.028\frac{t}{L^2}\sqrt{\frac{E}{\rho}} \quad (1.a)$$

$$k_0 = 16\frac{Et^3w}{L^3} \quad (1.b)$$

t,w and L are respectively the thickness, width and length of the micro-bridge. E and ρ are respectively the Young's modulus and density. The stiffness k_0 is defined here as the force to deflection ratio at the center of the bridge. Equations (1) lead to the classical relation between stiffness and resonance frequency:

$$f_{R0} = \frac{\alpha}{2\pi}\sqrt{\frac{k_0}{M}} \qquad (2)$$

where $M = \rho twL$ is the total mass and α a nondimensional geometrical parameter accounting for the mode shape. In the present situation, we deduce the value $\alpha=1.615$ from equations (1).

The stiffness and resonance frequencies are modified by the applied current and the corresponding axial stress. Two regimes must be considered depending on the level of this stress:

i - tensile stresses ($\sigma > 0$) and compressive stresses lower than the buckling threshold ($\sigma < 0$ and $|\sigma| < |\sigma_c|$),

ii - compressive stresses larger than the buckling threshold ($\sigma < 0$ and $|\sigma| > |\sigma_c|$).

The buckling threshold stress σ_c is given by the Euler equation [7]:

$$\sigma_c = -\frac{\pi^2 E t^2}{3L^2} \qquad (3)$$

1.2 Pre-buckling regime:

In the first regime, ie., for $\sigma > \sigma_c$, the flexural resonance frequencies are obtainable from the equation of the lateral vibrations of a bridge subjected to an axial load. The first frequency is given by the Galef's formula [8]:

$$f_R = f_{R0}\sqrt{1-\frac{\sigma}{\sigma_c}} \qquad (4)$$

where f_{R0} is given by equation (1.a).

1.3 Post-buckling regime:

In the post buckling regime, ie., for $\sigma < \sigma_c$, the Rayleigh-Ritz method could be applied for the obtention of the resonance frequencies [7]. This method leads to an approximate solution since it uses an assumption concerning trial functions for mode shapes. In the following, we have chosen to calculate the first bending resonance frequency through the bending stiffness, according to a relation similar to equation (2):

$$f_R = \frac{\alpha}{2\pi}\sqrt{\frac{k}{M}} \qquad (5)$$

The stiffness k in the post-buckling regime is derived from a load-deflection relationship obtained by an energy minimization method [9], and is given by the following approximate relation :

$$k = k_0 \frac{\pi^4}{24}\left(\frac{\sigma}{\sigma_c} - 1\right) \qquad (6)$$

where k_0 is given by equation (1.b).

Combination of equations (6), (5) and (2) leads to the following expression of post-buckling resonance frequency which is similar to the Galef's formula (equation 4):

$$f_R = 2.015 f_{R0}\sqrt{\frac{\sigma}{\sigma_c} - 1} \qquad (7)$$

2 - Temperature and stress variations induced by Joule heating:

By considering that thermal conduction is the dominating heat transfer phenomenon, the current-induced temperature distribution in a micro-bridge was calculated analytically in [10]. It leads to the following normalized form of the mean temperature increase:

$$\overline{\Delta T} = \begin{cases} \dfrac{1}{\xi}\dfrac{u-1}{u}\left\{\dfrac{th(\beta\sqrt{u})}{\beta\sqrt{u}} - 1\right\} & for\ I < I_0 \\ \dfrac{1}{\xi}\dfrac{u+1}{u}\left\{\dfrac{tan(\beta\sqrt{u})}{\beta\sqrt{u}} - 1\right\} & for\ I > I_0 \\ \dfrac{\beta^2}{3\xi} & for\ I = I_0 \end{cases} \qquad (8)$$

with $u = \left|1-(I/I_0)^2\right|$. ξ is the temperature coefficient of electrical resistivity. The parameters I_0 and β depend on the one hand, on the bridge dimensions and its thermal and electrical conductivities and, on the other hand, on the thermal conductivity of the surrounding air and the gap separation from the substrate.

The stress variation in the micro-bridge arising from thermal expansion is derived from the Hooke's law:

$$\Delta\sigma = -\frac{E\alpha\overline{\Delta T}}{3(1-2\nu)} \qquad (9)$$

The curves plotted in Fig.4 completely describe the behavior of a current-controlled monocrystalline silicon micro-bridge resonator whose dimensions are 500µm in length, 10µm in thickness and 4µm in width without initial stress ($\sigma_0 = 0$). These curves result from equations (4) and (7-9).

This first-order analytical model is based on the following approximations:

a) low vibrations amplitudes ($<t$) are considered;

b) it is assumed that the first bending resonance frequency in the post-buckling regime can be calculated from stiffness according to equation (5), in which the nondimensional

factor α has the same value as for a stress-free micro-bridge (α=*1.615*);
c) the analytical expression of this stiffness results from an approximation since the load-deflection relation has been derived on the basis on an energy minimization method [9];
d) for stress calculations, a uniform temperature is considered in the micro-bridge (equation (9)); this temperature is taken equal to the mean value of a temperature distribution which also results from approximations [10];
e) the model does not account for the strong interactions that may occur between electrical, thermal and mechanical phenomena.

In order to refine the first-order analytical model and to estimate its accuracy, FEM simulations have been performed. They are presented in the following section.

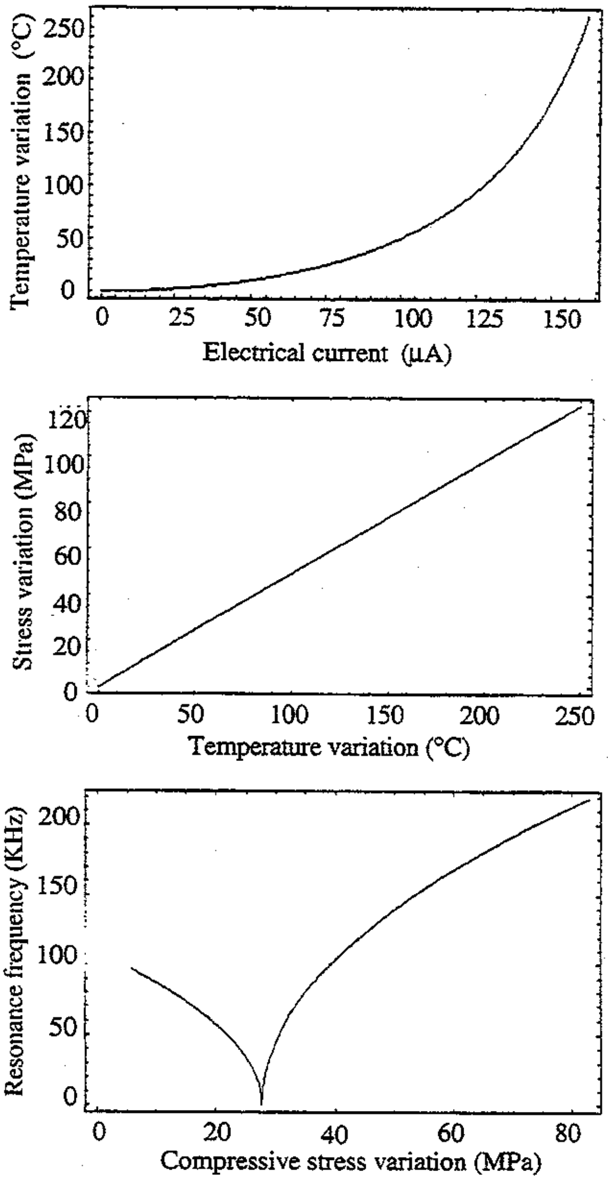

Figure 4
Analytical characteristics of a perfect silicon micro-bridge (500µm long, 10µm thick and 4µm wide)

FEM ANALYSIS AND REFINED MODEL

Although some quantities are obtainable from exact solutions in the case of a simple geometry like the considered micro-bridge, we will follow a procedure in which all calculations are performed in the FEM tool and which could be applied to other structures with non-trivial geometries, even with multiple materials. The complete FEM simulation procedure involves three steps:
1) - a buckling analysis for the extraction of the buckling threshold stress: from this analysis we deduce the stress ranges for the next simulations;
2) - a non-linear static analysis: this analysis gives the deflection-load characteristics, particularly in the post-buckling range. (These characteristics lead for example, to the displacement magnitude for actuator applications and to capacitance variations for sensors);
3) - a frequency modal analysis of the stressed micro-bridge resonator: this modal analysis is performed for each value of the axial load just after the corresponding non-linear static analysis.

The simulated structure is also a single-crystal silicon micro-bridge 500µm long, 10µm thick and 4µm wide. All simulations have been performed with an eight-node shell element (SHELL93).

1 - Buckling analysis

The first buckling mode and the corresponding eigen-buckling stress value are extracted. The latter is $\sigma_c = -27.6\ MPa$. As expected, it is in very good agreement with the value obtained from equation (3). This also corresponds to a critical temperature increase $\Delta T_c = 56\ °C$, according to equation (8). As mentioned above, this first FEM analysis is necessary for non-trivial geometries for which an analytical expression of the buckling threshold is not available.

2 - Non-linear static analysis

In order to evidence the buckling behavior and to make a quantitative analysis of the deflection under the application of an axial compressive load, a non-linear static analysis has been performed. The deflection-load characteristic for a perfect bridge is given by the following equations :

$$w_0 = \begin{cases} 0 & for\ \sigma > \sigma_c \\ \dfrac{2t}{\sqrt{3}}\sqrt{1-\dfrac{\sigma}{\sigma_c}} & for\ \sigma > \sigma_c \end{cases} \qquad (10)$$

This characteristic is plotted with a solid line in Fig.5. This plot shows a sharp deflection increase at the threshold buckling stress σ_c.

The FEM non-linear static analysis needs the application of a small transversal load to the bridge in addition to the axial load. The effect of this lateral load alone is to produce an initial deflection w_0. Such a deflection at the center of the bridge is generally considered to model imperfections of various nature, including geometrical irregularities, defects and nonuniform loading [10]. The higher the initial deflection, the smoother the deflection increase around the buckling threshold, as previously shown in the works of Fang *et al.* [11] and Saif *et al.* [6]. This effect is illustrated in Fig.5. It is noteworthy that a deflection of about 10µm is obtainable with a temperature increase of 240°C, which corresponds to a heating current of only 0.16 mA. Such a deflection is convenient for actuator applications.

In addition to the smoothing effect of the deflection-load characteristics around the buckling threshold σ_c, another consequence of imperfections is that the buckling mode degeneration is broken, that is, the bridge always buckles along a preferred direction.

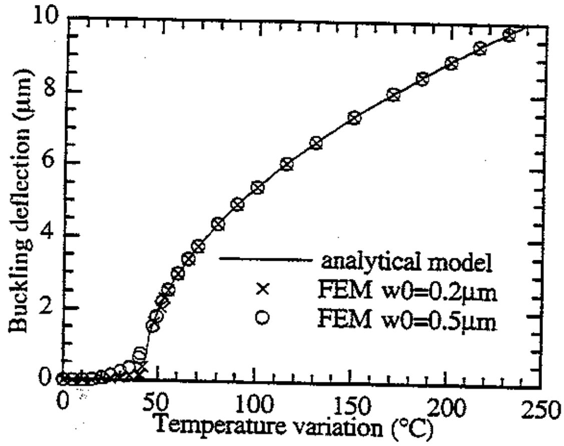

Figure 5
Micro-bridge buckling deflection versus temperature increase (analytical and FEM)

3 - Frequency modal analysis of strained resonators

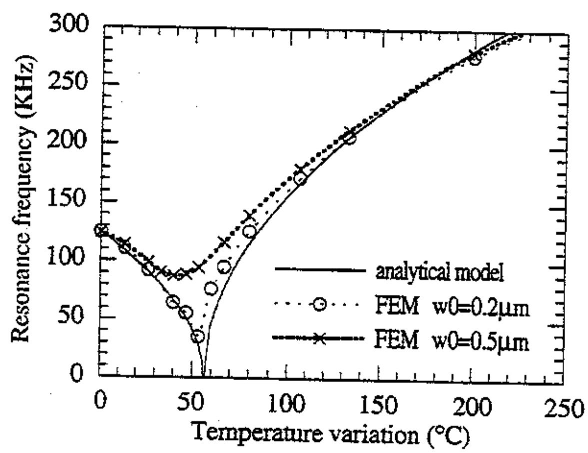

Figure 6
Resonance frequency versus temperature variation (analytical and FEM models)

A frequency modal analysis is then performed for each value of the axial load to extract the resonance frequencies and mode shapes of the strained structure. In order to analyze the effect of imperfections, these simulations are repeated for several values of the initial deflection w_0. The first resonance frequency is plotted in Fig.6. The results of the FEM simulations are superimposed with those of the analytical model (equations (4) and (7)). Circles and crosses are related to FEM results with an initial deflection of 0.2µm and 0.5µm respectively. One can see two important features from this figure: first, for an imperfect bridge, the resonance frequency does not vanish at the buckling threshold: the higher the initial deflection, the higher the minimum frequency; secondly, the position of this minimum shifts towards small compressive stresses when increasing the initial deflection.

4 - Refined models

Different FEM simulations have been performed on a silicon micro-bridge in order to have a more accurate description of its behavior. These simulations account for a new effect (imperfections) and lead to a first refined model. Starting from the simulations data, the parameters of the analytical model can be adjusted and new parameters can also be added. However, approximations remain in this model. Indeed, on the one hand, the axial load or what is equivalent, the current-induced temperature increase, is assumed to be uniform; on the other hand, coupling between electrical, thermal and mechanical domains has not been considred yet. We are currently working towards the development of a new FEM model with proper account of these phenomena.

SYSTEM-LEVEL SIMULATIONS

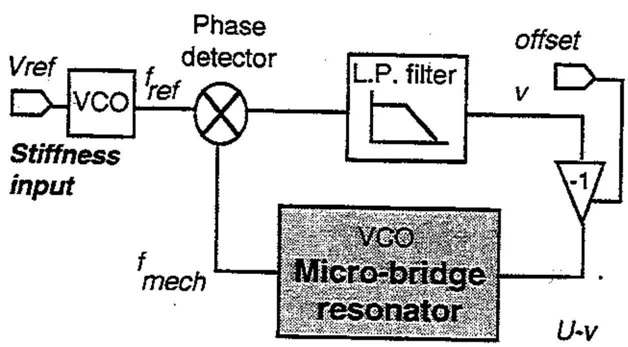

Figure 7
Electrical circuit for stiffness control

In order to perform a stiffness control, the resonance frequency of the micro-bridge is controlled in a Phase-Locked-Loop (PLL) circuit in which the Voltage Controlled Oscillator (VCO) is replaced by the micro-bridge resonator (Fig.7). The latter appears as a mechanical VCO and it is linked to other conventional electrical components to form a complete PLL. However, the structure of this PLL is somewhat unusual because of the strongly non-linear characteristic of the mechanical VCO (see Fig.4). Indeed, since the first branch of this characteristic corresponds to a frequency decrease with voltage (current), that is a negative equivalent VCO factor K_0, the whole system stability needs a transformation $V \rightarrow U - V$ between the low-pass filter and the VCO, where V designates the filter output and U an offset whose magnitude is lower than the buckling voltage. The reference frequency at the input of the PLL is generated with another VCO of electrical nature, so that a desired stiffness is controlled by the voltage at the input of this second VCO.

An example of simulation result is shown in Fig.8. This simulation corresponds to a step voltage at the input of the electrical VCO generating a frequency jump at the PLL input. A demonstration is given for the PLL locking for two values of the stiffness reference voltage.

Multi-level simulations have been performed to analyze a tunable microbridge resonator: analytical and FEM simulations at the device level, electrical/behavioral simulations at the system level. Models with different degrees of refinement can be used. This modeling/simulation procedure will now be used for the development of more complex systems employing such resonators.

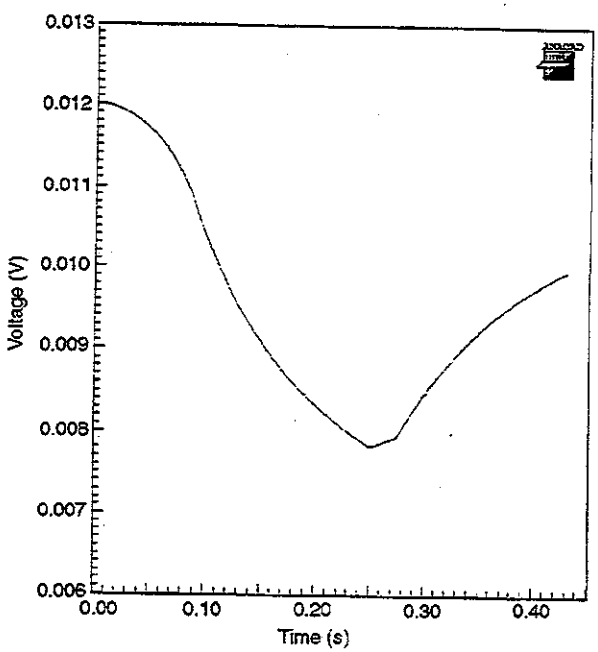

Figure 8

ACKNOWLEDGEMENTS

The authors would like to thank E.Donzier and J.P.Gilles for helpful discussions, P.Dollfus and F.X.Musalem and C.Arcile for their valuable help in this work.

REFERENCES

1- J.J.Yao, N.C.MacDonald "A micromachined, single crystal silicon, tunable resonator". J. Micromech. Microeng., 6, 1996, 257-264.

2- Y.Fukuta, T.Akiyama, H.Fujita "A Reshaping Technology with Joule Heat for Three Dimensional Micrr tructures". IEEE Conf. Solid State Sensors and Actu. ..ors (Transducers'95), Stockholm, Sweden, June 25-29, (1995) 174-177.

3- T.Akiyama H.Fujita "A quantitative analysis of scratch-drive actuator using buckling motion". MEMS'95 310-315.

4- B.Wagner, H.J.Quenzer, S.Hoerschelmann, T.Lisec, M.Juerss "Bistable Microvalve with pneumatically coupled membranes". MEMS'96 384-388.

5- J.Gobet, F.Cardot, J.Bergqvist, F.Rudolf "Electrodeposition of 3D microstructures on silicon". J. Micromech. Microeng. 3 (1993) 123-130.

6- M.T.A.Saif, N.C.MacDonald "A Millinewton Microloading Device". Sensors and Actuators. vol A52 (1996) 65-75.

7- S.Rao "Mechanical vibrations" Third edition Addison-Wesley publishing (1995).

8- A.E.Galef "Bending frequencies of compressed beams". Journal of Acoustical Society of America. 44(8) 643 (1968) in A.Bokaian "Natural frequencies of beams under compressive axial loads". Journal of Sound and Vibration. 126 (1) 49-65 (1988).

9 - J.Haji-Babaei, C.Y.Kwok, R.S.Huang "Buckling behaviour of electrostatically actuated doubly-supported beams". 11th European Conference on Solid State Transducers, EUROSENSOR XI, september 21-24 (1997), Warsaw, Poland.

10 - L.Lin,M.Chiao "Electrothermal responses of lineshape microstructures". Sensors and Actuators. A55 (1996) 35-41.

11 - W.Fang, J.A.Wickert "Post buckling of micromachined beams". Journal of Micromechanics and microengineering. 4 (1994) 116-122.